ANNALS of Clinical and Translational Neurology
Open Access
ANA American Neurological Association since 1875

Advanced MRI unravels the nature of tissue alterations in early multiple sclerosis

Guillaume Bonnier[1,2,3], Alexis Roche[1,3,4], David Romascano[1,3], Samanta Simioni[2], Djalel Meskaldji[3], David Rotzinger[4], Ying-Chia Lin[5], Gloria Menegaz[5], Myriam Schluep[2], Renaud Du Pasquier[2], Tilman Johannes Sumpf[6], Jens Frahm[6], Jean-Philippe Thiran[3], Gunnar Krueger[1,7] & Cristina Granziera[1,2,3]

[1]Advanced Clinical Imaging Technology group, Siemens Healthcare IM BM PI, Lausanne, Switzerland
[2]Neuro-immunology and Laboratoire de recherché en neuroimagérie, Neurology Division, Department of Clinical Neurosciences, Centre Hospitalier Universitaire Vaudois and University of Lausanne, Lausanne, Switzerland
[3]LTS5, Ecole Polytechnique Fédérale de Lausanne, Lausanne, Switzerland
[4]Department of Radiology, Centre Hospitalier Universitaire Vaudois and University of Lausanne, Lausanne, Switzerland
[5]Department of Computer Science, University of Verona, Verona, Italy
[6]Biomedizinische NMR Forschungs GmbH, Max Planck Institute for Biophysical Chemistry, Goettingen, Germany
[7]Healthcare Sector IM&WS S, Siemens Schweiz AG, Renens, Switzerland

Correspondence
Cristina Granziera, Department of Clinical Neurosciences, Neurology, CHUV, 1011 Lausanne, Switzerland. Tel: +41 79 5565687; Fax: +41 21 3141291; E-mail: cristina.granziera@chuv.ch

Funding Information
The Swiss National Science Foundation under grants PZ00P3_131914/11, PP00P2-123438; the Swiss MS Society and the Societé Académique Vaudoise.

Received: 12 February 2014; Revised: 27 March 2014; Accepted: 28 April 2014

Annals of Clinical and Translational Neurology **2014; 1(6): 423–432**

doi: 10.1002/acn3.68

Abstract

Introduction: In patients with multiple sclerosis (MS), conventional magnetic resonance imaging (MRI) provides only limited insights into the nature of brain damage with modest clinic-radiological correlation. In this study, we applied recent advances in MRI techniques to study brain microstructural alterations in early relapsing-remitting MS (RRMS) patients with minor deficits. Further, we investigated the potential use of advanced MRI to predict functional performances in these patients. **Methods**: Brain relaxometry (T1, T2, T2*) and magnetization transfer MRI were performed at 3T in 36 RRMS patients and 18 healthy controls (HC). Multicontrast analysis was used to assess for microstructural alterations in normal-appearing (NA) tissue and lesions. A generalized linear model was computed to predict clinical performance in patients using multicontrast MRI data, conventional MRI measures as well as demographic and behavioral data as covariates. **Results**: Quantitative T2 and T2* relaxometry were significantly increased in temporal normal-appearing white matter (NAWM) of patients compared to HC, indicating subtle microedema ($P = 0.03$ and 0.004). Furthermore, significant T1 and magnetization transfer ratio (MTR) variations in lesions (mean T1 z-score: 4.42 and mean MTR z-score: −4.09) suggested substantial tissue loss. Combinations of multicontrast and conventional MRI data significantly predicted cognitive fatigue ($P = 0.01$, Adj-$R^2 = 0.4$), attention ($P = 0.0005$, Adj-$R^2 = 0.6$), and disability ($P = 0.03$, Adj-$R^2 = 0.4$). **Conclusion**: Advanced MRI techniques at 3T, unraveled the nature of brain tissue damage in early MS and substantially improved clinical–radiological correlations in patients with minor deficits, as compared to conventional measures of disease.

Introduction

Multiple sclerosis (MS) is an inflammatory and neurodegenerative disease of the central nervous system (CNS) characterized by the presence of focal lesions in white matter (WM) and gray matter (GM) and also by diffuse inflammation and degeneration in normal-appearing (NA) tissue.[1,2] Conventional MRI plays a major role in identifying focal inflammation and diagnosing MS, but has important limits in assessing underlying pathology. As a consequence, this method provides only modest correlations with patient functional performance, particularly during early phases of the disease.[3]

In this context, quantitative and semiquantitative (q/sq) MRI techniques[4,5] may provide new biomarkers of disease severity and help to improve the clinical–radiological mismatch in MS treatment. To this end, pathological processes such as demyelination, edema formation, tissue

loss, and iron accumulation lead to variable changes in quantitative measures of proton relaxation times (T1, T2, and T2*) as well as in semiquantitative parameters such as the magnetization transfer ratio (MTR).[6–10] Thanks to recent MRI developments,[11,12] it is now possible to combine multiple q/sq MRI sequences in a clinically applicable protocol and gather more specific information about the nature of tissue pathology in MS.

In this work, we investigated whether the combination of advanced T1, T2, and T2* relaxometry and magnetization transfer imaging may be employed (1) to assess the nature of brain tissue changes occurring early in MS and (2) to improve the correlation between imaging and clinical performance.

Methods

Study population

We enrolled 36 patients with relapsing-remitting MS (RRMS), 24 women/12 men, age = 34.8 ± 9.2 years (mean ± standard deviation [SD]) and 18 age-matched healthy controls (HC), 9 women/9 men, age = 33 ± 9.7 years. All patients were <6 years from initial symptoms (33.3 ± 21 months, range 2–70 months) and disease diagnosis (27.1 ± 18 months, range 0–59 months). Thirty patients (83%) were under immunomodulatory treatment (high dosage interferon beta or fingolimod) for at least 3 months. No patient had received corticosteroid therapy within the 3 months preceding the enrollment. The study was approved by the ethics committee of the Lausanne University Hospital (CHUV). Written, informed consent was obtained from each subject.

Clinical assessment

Each subject underwent a neurological examination including the following cognitive and behavioral tests: (1) Brief Repeatable Battery of Neuropsychological Tests (BRB-N),[13] which examine verbal and spatial memory, sustained attention, information processing speed, and verbal fluency on semantic cues; (2) the Hospital Anxiety and Depression scale (HAD)[14]; and (3) the Fatigue Scale for Motor and Cognitive functions (FSMC),[15] which quantifies depressive mood symptoms and fatigue. The Expanded Disability Status Scale (EDSS[16]) and the Multiple Sclerosis Functional Composite (MSFC[17]) scores were assessed by a certified neurologist (C. Granziera, CG) to quantify motor performance.

MRI techniques

All MR images were acquired on a 3T Siemens Trio (Siemens, Erlangen, Germany) equipped with a 32-channel head coil. The acquisition protocol consisted of: (1) high-resolution 3D magnetization-prepared acquisition with gradient echo (MPRAGE) (TR/TE = 2300/2.98 ms, voxel size = 1.0 × 1.0 × 1.2 mm^3, FoV = 256 × 240 × 192 mm^3, acquisition time = 5:12 min) for automatic brain tissue, and atlas-based segmentation as reported previously[18–20]; signal-to-noise ratio (SNR) measurements on a MPRAGE image were performed based on[21,22] and reported in detail in the supplementary data (2) high-resolution 3D fluid attenuated inversion recovery (FLAIR) (TR/TE/TI = 5000/394/1800 ms, voxel size = 1.0 × 1.0 × 1.2 mm^3, FoV = 256 × 240 × 212 mm^3, acquisition time = 6:27 min); (3) high-resolution 3D double inversion recovery (DIR) (TR/TE/TI = 10,000/218/3650 ms, voxel size = 1.1 × 1.0 × 1.2 mm^3, FoV = 256 × 240 × 192 mm^3, inversion times 450/3652 ms, acquisition time = 12:52 min); (4) Magnetization-Prepared 2 Rapid Acquisition Gradient Echoes MP2RAGE[12] (TR/TE = 5000/2.89 ms, voxel size = 1.0 × 1.0 × 1.2 mm^3, FoV = 256 × 240 × 212 mm^3, acquisition time = 8:22 min) for lesion count,[23] and whole-brain T1 relaxometry; (5) T2 relaxometry (TR/TE = 5850/9 ms, 21 echos, 30 slices: voxel size = 1.0 × 1.0 × 4.0 mm^3, FoV = 210 × 175 × 120 mm^3, acquisition time = 3 min) using a new nonlinear inverse reconstruction algorithm that directly estimates a T2 and spin-density map from a train of undersampled spin echoes[11]; and finally, (6) T2* relaxometry (TR/TE = 47/1.23 ms, 32 gradient echoes, voxel size = 1.6 × 1.6 × 1.6 mm^3, FoV = 217 × 217 × 179 mm^3, acquisition time = 11:16 min) with and without magnetization transfer (MT) pulse (MT pulse flip angle: 220°; duration: 4000 ms; pulse offset: 2000 Hz; spoiler moment: 25,000 us × mT/m[24]). In order to correct for susceptibility induced macroscopic field inhomogeneities, which were already diminished by isotropic high-spatial resolution, we used a 3D Sinc Correction[25] that was extended to include a nonlinear correction term based on the underlying B0 map[26]; The B0 map was calculated as the weighted mean phase difference[27] of the temporally unwrapped phase followed by a median and Gaussian filters to remove phase inconsistencies.[28] R2′ maps were computed from T2 and T2* maps according to

$$R2' = \frac{1}{T2^*} - \frac{1}{T2}$$

MTR maps were derived from the T2* data by

$$\mathrm{MTR} = \frac{M_0 - M_T}{M_0}$$

with M_0 and M_T the images acquired without and with MT pulse, respectively. MT images were registered to images without MT pulse. Before any processing, image quality was assessed for each modality by visual inspection.

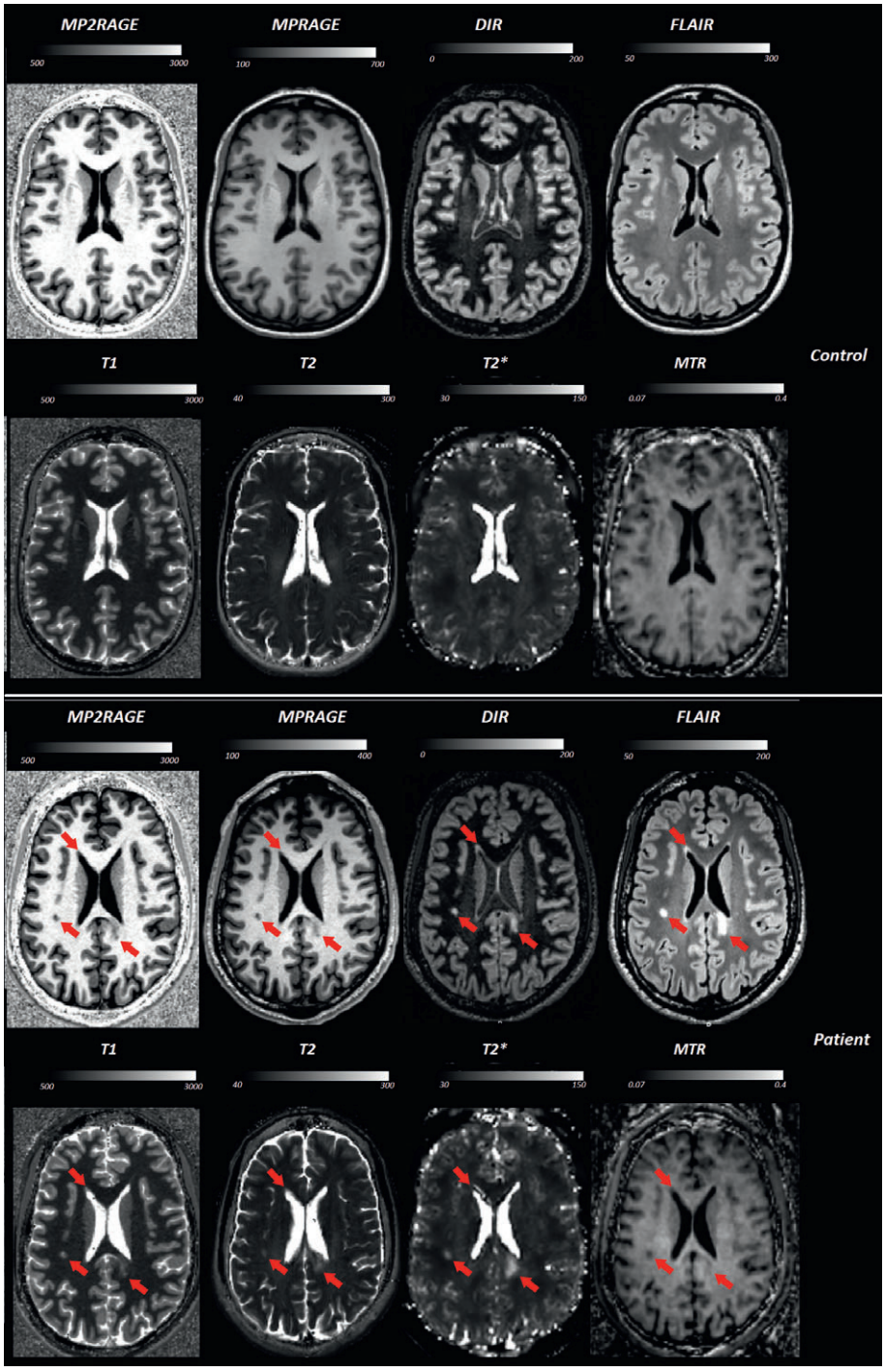

Figure 1. MP2RAGE uniform image, MPRAGE, DIR, 3D FLAIR images as well as MP2RAGE T1, T2, T2*, and MTR maps for one healthy control subject (first two raws) and one MS patient (last two raws). Examples of lesions are shown by red arrows in the images from the MS patient.

Figure 1 provides an example of all images and maps in one HC and one MS subject.

Raw data from a HC are available in Data S1.

Total scan time was ~47 min.

MRI contrasts

T1 relaxation time (rt) in brain tissue is mainly influenced by free water protons and the degree of structural

organization (i.e. amount of macromolecules such as myelin, lipids, proteins). In this context, an increase in T1rt may indicate a loss of structure and/or an increase in water content. Conversely, greater density of macromolecules and reduced water content as well as iron accumulation tend to reduce T1.[29]

T2rt measures the loss of spin coherence, and therefore, mainly reflect the dynamic state of water protons and their interaction with macromolecules. An increase in T2rt characterizes a loss of macromolecules and/or increased water content. On the contrary, a decrease in T2rt reflects an increase in protons bound to macromolecules. As for T1, iron accumulation also causes a shorter T2[30] (Fig. 1).

The effective T2* transverse rt describes the loss of transverse magnetization due to T2 relaxation and magnetic field inhomogeneities (R2′ component[31]). Possible sources are tissue-dependent differences in magnetic susceptibility or the presence of paramagnetic or ferromagnetic ions like iron. For these reasons, an increase in T2* most often indicates a loss of macromolecules, while a decrease suggests an increase in macromolecular compounds or iron that translate into an increase in R2′.

MT images are based on the interaction between free protons and immobilized protons bound to macromolecules, so that a lower MTR indicates a reduced spin exchange between macromolecules and surrounding bulk water suggesting neuroaxonal damage or myelin breakdown[32] and/or water increase.

Image analysis and tissue segmentation

We used the Elastix c++ library[33] to perform (1) rigid registration with BSpline interpolation of the T2 maps to the T1 maps (from the MP2RAGE); and (2) rigid registration of T2* maps, MPRAGE, FLAIR, and DIR images to one of the inverted contrasts of the MP2RAGE sequence. By doing this, we obtained all images in the MP2RAGE space.

Regions of interest (ROIs) were derived from the MPRAGE image using in-house software based on variational expectation-maximization tissue classification.[34] The following ROIs were automatically segmented: whole-brain WM and cortical GM, thalamus, and basal ganglia (caudate, putamen, and globus pallidus), cerebellar WM and GM. In addition, we computed lobar WM and GM (temporal, occipital, frontal, parietal areas).

An experienced neurologist (CG) and a radiologist (D. Rotzinger, DR) manually counted MS lesions by consensus in 3D FLAIR, 3D DIR, and MP2RAGE images for all MS subjects and HC, as performed previously.[20] A trained technician generated manual contours for each lesion in the three different contrasts (rechecked by DR). In order to maximize the sensitivity of lesion count and volume, lesion masks from each contrast were merged into a single mask (lesion union mask), as reported by Kober et al.[20]

The lesion union mask and the ROIs masks were then registered to the T1, T2, T2*, and MTR maps to obtain parametric values in lesions and NA tissue in each ROI.

The volume of each ROI was also automatically obtained using the in-house software based on a previous report[34] and normalized by total intracranial volume.

Statistical analyses

Between-groups comparisons of subjects' demographics and clinical scores

Differences in age, gender, education, and clinical performance were assessed using a nonparametric ANOVA (Kruskal–Wallis test) among HC and MS patients.

Between-groups comparisons of multicontrast MRI data

To assess NA tissue differences in mean T1, T2, T2*, and MTR of patients and controls, we performed a permutation-based Hotelling test with 10,000 permutations, age and gender as covariates, and family-wise correction for multiple comparisons.

The following null hypotheses were tested: (1) there are no differences in WM and GM of temporal, parietal, occipital, and frontal lobes; (2) there are no differences in cerebellum WM and GM; and (3) there are no differences in thalamus and basal ganglia.

Lobar assessment was chosen, instead of whole brain, to take into account the local variation in quantitative relaxometry measures, as reported previously.[35,36]

In order to determine the strength of the significance, we also calculated the *Cohen's d* effect size as follow:

$$d = \frac{\bar{x}_1 - \bar{x}_2}{s}$$

with $\bar{x}_1$ and $\bar{x}_2$ the mean of the group 1 (HC) and group 2 (RRMS), and s defined as follows:

$$s = \sqrt{\frac{(n_1 - 1)s_1^2 + (n_2 - 1)s_2^2}{n_1 + n_2 - 2}}$$

Parameters s_1 and s_2 refer to the standard deviation of group 1 (HC) and group 2 (RRMS), while n_1 and n_2 are the number of samples of group 1 and 2.

In order to compare lesional tissue, MRI properties in patients with the corresponding healthy tissue in HC, we calculated a z-score for each lesion and then averaged the

lesion z-scores across all lesions in each subject as follows (i.e. for T1 data):

$$z_{T1} = \frac{1}{N} \sum_{l \in \{Lesions\}} \sum_{v \in l} \frac{I_{T1}(v) - \mu_{T1}(L_l, T_l)}{\sigma_{T1}(L_l, T_l)}$$

where z_{T1} corresponds to the average of T1 lesion z-scores in one patient, N to a normalization term, I_{T1} the T1 map, $\mu_{T1}(L_l, T_l)$ and $\sigma_{T1}(L_l, T_l)$ to the mean and the standard deviation of T1 in the lobe L_l and tissue T_l (i.e. WM or GM) in the HC group, corresponding to the lesion location. Averages of each patient's T1, T2, T2*, and MTR lesion z-scores were also performed in the whole MS group.

This approach was chosen instead of the permutation-based test applied for NA tissue to account for spatial variation in relaxometry values.[35,36] A permutation test was not feasible for each lobe as not all patients exhibited lesions in all lobes.

Between-groups comparison of volumes

To assess volumetric differences in ROIs' between patients and controls, we performed a permutation-based Hotelling test with 10,000 permutations, age and gender as covariates, and family-wise correction for multiple comparisons.

Linear regression of MRI parameters with clinical scores

All regression analyses were performed using R software (http://www.R-project.org).

A multivariate linear regression of clinical scores was performed using a general linear model (GLM) applied (1) T2*, T2, T1, and MTR in the ROIs that differed between patients and HC, (2) T1, T2, T2*, and MTR lesion z-scores and (3) cortical/subcortical lesion count and volume. Age, gender, educational years, anxiety, and depression scores (HAD) were considered as covariates, since they have been reported to be linked to functional performance.[37,38] Cognitive scores were adapted using Box–Cox transformation to satisfy model assumption for normality.[39] EDSS scores were not considered, as they were positive only in patients.

We performed seven regressions, where we used a backward stepwise approach to select the best prediction model for each dependent variable (clinical scores). Bonferroni correction was applied for multiple comparisons (seven tests).

Cook's distance (Cd) was computed to assess the influence of each observation on the regression process, using $4/n$ (n: number of observations) as the threshold of significance. Robust regression was used to reduce influence of the outliers identified by Cook's distance analysis. "Leave-one-out" (LOO) cross-validation was applied to assess the prediction quality and robustness of each model. A $P < 0.05$ was considered statistically significant.

Results

Between-groups comparisons of subject demographics and clinical scores

No significant differences were observed between HC and MS patients in terms of age ($P = 0.3$) or gender ($P = 0.8$); however, HC had slightly higher education levels (17 $\pm$ 4 years, mean $\pm$ standard deviation) than MS patients (15 $\pm$ 3 years, $P = 0.04$).

Mean EDSS in patients was 1.6 $\pm$ 0.3 (interval: 1–2). The FSMC motor score was significantly higher in MS patients (23.1 $\pm$ 10.5) than in HC (14.8 $\pm$ 5.8, $P < 0.02$). The FSMC cognitive scores, cognitive performance, MSFC scores, as well as anxiety and depression scores (HAD) were not significantly different between groups ($P > 0.1$).

Between-groups comparison of multicontrast MRI data

In temporal NAWM, mean T2* and T2 were significantly higher in RRMS patients compared to HC (T2* rt: 55.1 $\pm$ 1.55 msec in patients and 53.4 $\pm$ 1.35 msec in HC, $d = 1.17$, $P = 0.004$, Fig. 2; T2 rt: 82.0 $\pm$ 2.38 msec in patients and 79.8 $\pm$ 2.0 msec in HC, $d = 1$, $P = 0.03$, Fig. 2).

In order to assess whether the observed T2* increase in temporal NAWM depended on local field inhomogeneities, we also compared temporal NAWM R2′ between groups and found no significant differences.

Additionally, parietal NAWM and cerebellar NAWM exhibited a trend toward higher T2 values in patients compared to HC (parietal NAWM T2: 83.5 $\pm$ 2.44 msec in patients compared to 81.8 $\pm$ 2.62 msec in HC; $d = 0.7$, $P = 0.05$; and cerebellar WM T2: 85.90 $\pm$ 1.69 msec in patients compared to 85.48 $\pm$ 1.47 msec in HC; $d = 1.62$, $P = 0.07$).

Further, no differences were seen for T1 and MTR in NAWM and cortical NAGM, nor for T2 and T2* in cortical NAGM, frontal or occipital NAWM. Finally, no significant differences between groups were found for T1, MTR, T2, or T2* in the thalamus or basal ganglia.

Results of microstructural analysis of lesions are reported in Figure 3.

In the MS cohort, MS lesions showed a strong increase in T1 mean z-score (4.42) and an important decrease in MTR mean z-score (−4.09). T2 and T2* mean z-scores slightly increased (2.33 and 2.25, respectively).

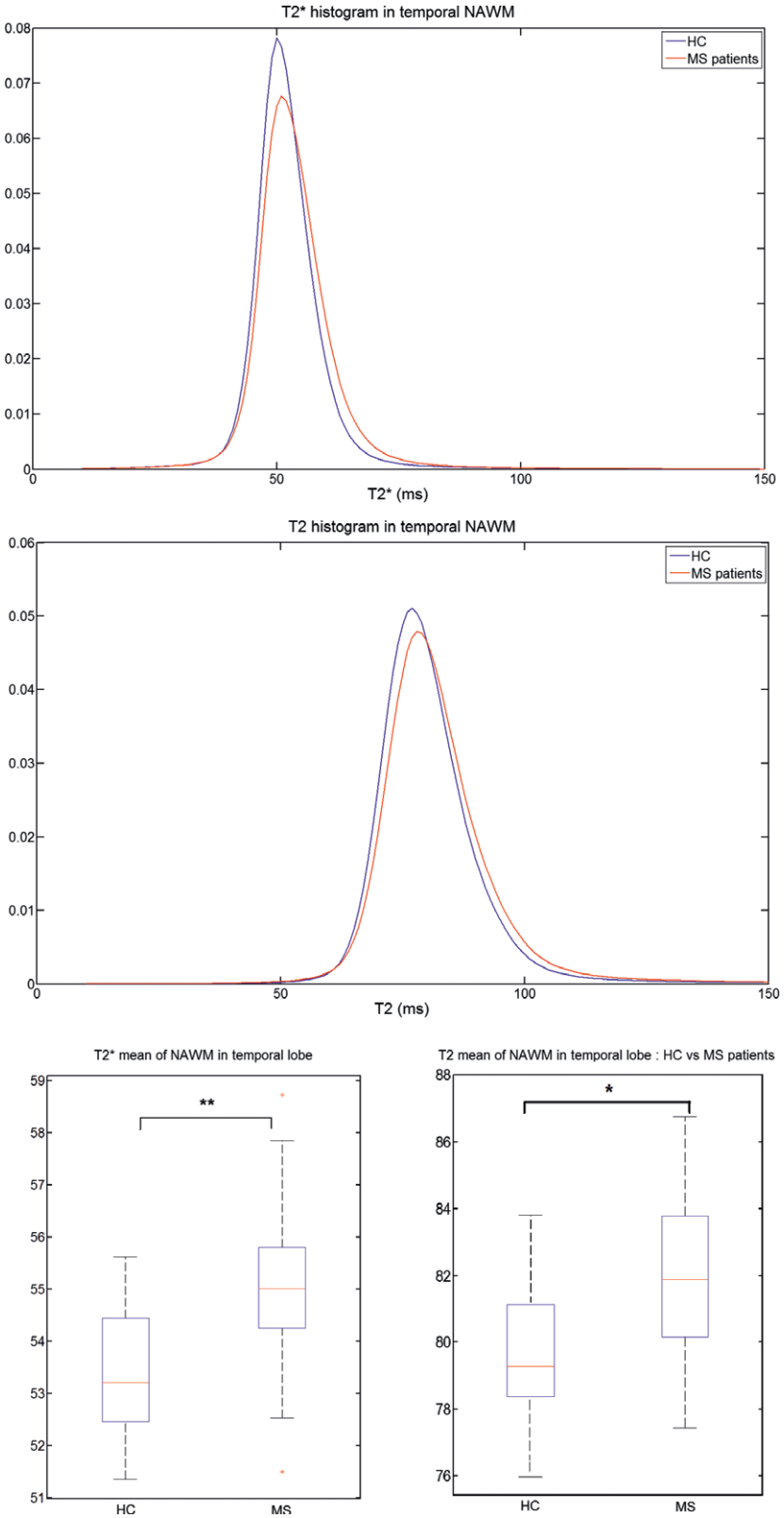

Figure 2. (A) (Top): T2* and T2 mean histograms in NAWM (temporal lobe) for HC (blue) and MS patients (red); (B) (Below): Boxplot of T2* and T2 in NAWM (temporal lobe) for HC (left) and MS patients (right).

Between-groups comparison of volumes

No significant differences were observed in volumes between MS patients and HC, however, there was a trend toward smaller normalized thalamic volumes in patients (absolute volume 15.31 ± 1.36 mm^3, normalized volume 0.01 ± 0.0006) compared to HC (absolute volume 16.52 ± 2.04 mm^3, normalized volume 0.01 ± 0.0003 $P = 0.07$).

Linear regression of MRI parameters with clinical scores

GLM using backward, stepwise regression revealed a highly significant association, confirmed by cross-validation results, between multicontrast MRI features and four clinical scores (Table 1):

1 Cortical lesions count and volume, T1, T2, and T2* mean z-score of lesions, T1, T2*, and MTR mean of temporal NAWM together with gender predicted the Symbol Digit Modalities Test (attention function) score (adjusted R2: 0.6, $P = 0.0005$).
2 T2, T2*, and MTR mean in temporal NAWM in conjunction with T1 and T2 mean z-score in lesions as well as subcortical lesion volume and educational years, gender and HAD scores predicted the MSFC (general disability) score (adjusted R2: 0.4, $P = 0.03$).
3 T1 and T2 mean in temporal NAWM combined with cortical lesion volume, subcortical lesion count, and

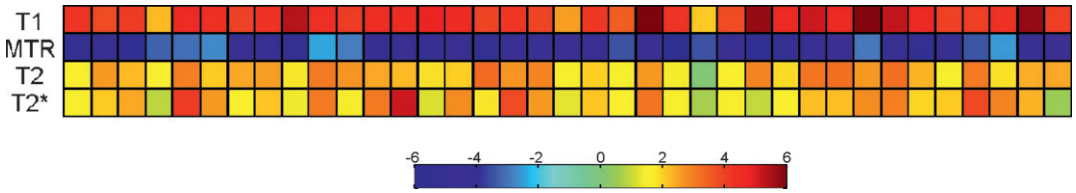

Figure 3. T1, MTR, T2, and T2* mean z-scores per patient (columns) in MS lesion.

Table 1. Multiple regression analysis between lesional and temporal NAWM MRI characteristics, covariates, and clinical scores.

		Clinical scores	*SDMT*	*MSFC*	*FSMCCog*	*FSMCMotor*	*Disease Duration*	*WLG*	*10/36*	*SRT*
Stepwise regression		p-value	0.00006	0.00397	0.00197	0.00156	0.00589	0.01748	0.02043	0.00999
		Corrected p-value	0.00051	0.03178	0.01577	0.01250	0.04708	0.13984	0.16344	0.07995
		Adjusted-R	0.59	0.43	0.36	0.42	0.35	0.13	0.29	0.32
Cross validation		p-value	0.00001	0.00010	0.00087	0.00145	0.16720	0.09650	0.11650	0.02650
		Corrected p-value	0.00004	0.00080	0.00696	0.01160	1.33760	0.77200	0.93200	0.21200
		Adjusted-R	0.44	0.24	0.26	0.24	0.03	0.05	0.04	0.11
Predictors (p-value)										
Conventional	Lesion	Cortical Volume	0.0036		0.0434	0.0219	0.0984			
		Cortical count	0.0022				0.0467			0.0870
		Subcortical volume		0.1418		0.1048				
		Subcortical count			0.0426	0.0005	0.0009		0.0166	0.0956
New & Covariates		T1 zscore	0.0025	0.0811						0.0009
		T2 zscore	0.0073	0.0806			0.0349		0.1706	0.0345
		T2* zscore	0.0188			0.0857	0.0327		0.0433	
		MTR zscore					0.2129			
	Temporal NAWM	T1 mean	0.0607		0.0024	0.0001				
		T2 mean		0.0377	0.0068	0.0089				0.0011
		T2* mean	0.0006	0.0245					0.0042	0.0007
		MTR mean	0.0004	0.0201					0.0153	
	Covariates	Age								
		Gender	0.0395	0.0010			0.0436	0.0175	0.0152	
		Educational years		0.0986						
		HADA (anxiety)		0.2009					0.1972	0.0609
		HADD (Depression)		0.0330	0.0072	0.0969			0.0638	

p < 0.001
p < 0.01
p < 0.05

Top part: each line corresponds to the *P*-values, corrected *P*-values, and adjusted-R^2 of each model ($n = 7$) subjected to regression and cross-validation analysis. Bottom part: each line corresponds to the *P*-values of each predictor for every regression model performed. The color scheme signifies the difference in significance: dark orange = highest significance ($P < 0.001$), light orange = middle range significance ($P < 0.01$), and yellow = low significance ($P < 0.05$).

HADD score predicted the FSMC cognitive score (adjusted R2: 0.4, $P = 0.01$).

4 T1 and T2 mean in temporal NAWM combined with cortical lesion volume, subcortical lesion count, and volume with HADD score predicted the FSMC motor score (adjusted R2: 0.4, $P = 0.01$).

Discussion

The present results demonstrate that combining multiple advanced MRI techniques, it is possible to unravel the nature of subtle tissue alterations in early MS. Moreover, MRI markers of inflammation and neurodegeneration may substantially improve clinical–radiological correlations compared to conventional measures.

The RRMS patients enrolled in our study exhibited significant increases in T2 and T2*rt in temporal NAWM, and to a lesser extent in parietal and cerebellar NAWM. These changes hint to an accumulation of extracellular water (microedema) and/or a reduction in macromolecular content (myelin) in affected brain tissue (Fig. 2). In the absence of significant changes in MTR and T1rt, which would support the structural explanation, the increase in both T2 and T2*rt most likely indicates the presence of subtle edema. Iron loss might also be responsible for a prolongation of T2 and T2*rt, but appears to be a less probable cause as no differences were observed in R2′, which reflects local field inhomogeneities.[40]

By combining multiple q/sq MRI measures, our study confirms work reporting T2 increase in NAWM in early MS[6,41] and extends these findings by providing new insights into the pathology underlying those changes. However, our data contradict studies showing a measured unimodal MTR decrease in NAWM of early MS patients attributed to myelin loss.[42,43] These studies focused mainly on untreated patients and applied MT imaging at lower spatial resolution and lower field strength (1.5 T) than ours. Furthermore, unimodal MTR studies in MS should be considered with caution, as MT imaging alone cannot discriminate between myelin alterations and variation in water content in tissues.[44]

Axonal degeneration in NAWM of early MS patients was also suggested by unimodal diffusion tensor imaging (DTI) studies, showing reduced fractional anisotropy (FA).[45,46] Nevertheless, this interpretation may be misleading since a decrease in anisotropy can derive from the loss of the branched-shape of microglia cells that is typical of their activated-inflammatory form.[47] Thus, another possible explanation is that reduced FA might point to inflammatory rather than degenerative phenomena.

Several studies tried to address the limitation of unimodality studies by combining T2 relaxometry, MTR measurements,[48] and DTI[49]; however, these studies focused on selected brain structures (i.e. corpus callosum[49] and corticospinal tract[48]) in patients with advanced stages of MS.[49] Our approach overcomes the above-mentioned limits by performing a whole-brain analysis of multiple q/sq assessments in early MS.

Our data also showed that both cortical and subcortical lesions were characterized by a strong increase in T1rt and decrease in MTR with relatively modest positive variations of T2 and T2*rt (Fig. 3). These findings are consistent with previous MRI literature[50,51] and histopathological studies[9,10,52] showing significant neurodegeneration in MS plaques.

No significant microstructural alterations were found in NA tissue belonging to the basal ganglia or thalamus in our MS cohort. Still, volumetric analyses revealed a trend toward lower regional volumes in patients ($P = 0.07$), which is consistent with thalamic atrophy reported in larger and more heterogeneous patient groups.[53]

Last, we showed that MRI findings of microstructural alterations in NA tissue and lesions substantially improved the clinical–radiological correlation obtained with conventional measures, even in the presence of minor functional deficits. In fact, a variable combination of relaxometry and MTR values significantly ameliorated the prediction of cognitive performance (attention), cognitive fatigue, and general disability obtained with traditional measures of disease burden and patient covariates (Table 1).

Conventional MRI measures of MS disease impact provide only modest correlations with clinical performances, a phenomenon that is known as the clinico-radiological paradox. Multivariate analyses and multicontrast, tract-specific measures were proposed to alleviate this paradox,[48,49] but suffered from the limitations of conventional protocols and partial brain analyses. Recently, ultra-high field MRI at 7 T has been used to identify subtypes of cortical lesions, whose numbers showed good correlations with disability and cognitive performance in MS.[54] Extending such work, the multicontrast approach presented here emerges as a whole-brain MRI method at a clinically-compatible magnetic field, which produces strong clinical-radiological correlations for both cognition and disability.

Future developments should aim at reducing the number of sequences required for optimal lesion detection (i.e. MP2RAGE and 3DFLAIR[23]) as well as at applying accelerated T1-T2* relaxometry sequences to achieve a well-suited protocol for the clinical workflow.

In summary, combining multiple recent MRI techniques at 3T we found (1) increased T2 and T2* in temporal NAWM, suggesting subtle microedema; (2) a strong increase in T1rt and decrease in MTR in lesions, indicating prevalent tissue degeneration; and (3) improved correlations between MRI data and measures of cognition and disability in early and minimally impaired MS patients. Additional studies extending the current methods to

patients at later disease stages and containing larger cohorts will be necessary in the future.

Acknowledgments

We thank S. Kannengiesser, P. Falkovskiy, and M. Babayeva for the computation of MPRAGE SNR maps.

Conflict of Interest

Dr A. Roche and G. Krüger work for Siemens AG Schweiz.

References

1. Filippi M. Multiple sclerosis: a white matter disease with associated gray matter damage. J Neurol Sci 2001;185:3–4.
2. Calabrese M, Filippi M, Gallo P. Cortical lesions in multiple sclerosis. Nature Rev Neurol 2010;6:438–444.
3. Rocca MA, Messina R, Filippi M. Multiple sclerosis imaging: recent advances. J Neurol 2013;260:929–935.
4. Deoni SC. Magnetic resonance relaxation and quantitative measurement in the brain. Methods Mol Biol 2011;711: 65–108.
5. Alexander AL, Hurley SA, Samsonov AA, et al. Characterization of cerebral white matter properties using quantitative magnetic resonance imaging stains. Brain Connect 2011;1:423–446.
6. Neema M, Goldberg-Zimring D, Guss ZD, et al. 3 T MRI relaxometry detects T2 prolongation in the cerebral normal-appearing white matter in multiple sclerosis. NeuroImage 2009;46:633–641.
7. Catalaa I, Grossman RI, Kolson DL, et al. Multiple sclerosis: magnetization transfer histogram analysis of segmented normal-appearing white matter. Radiology 2000;216:351–355.
8. Bakshi R, Benedict RH, Bermel RA, et al. T2 hypointensity in the deep gray matter of patients with multiple sclerosis: a quantitative magnetic resonance imaging study. Arch Neurol 2002;59:62–68.
9. Levesque IR, Giacomini PS, Narayanan S, et al. Quantitative magnetization transfer and myelin water imaging of the evolution of acute multiple sclerosis lesions. Magn Reson Med 2010;63:633–640.
10. Tardif CL, Bedell BJ, Eskildsen SF, et al. Quantitative magnetic resonance imaging of cortical multiple sclerosis pathology. Mult Scler Int 2012;2012:742018.
11. Sumpf TJ, Uecker M, Boretius S, Frahm J. Model-based nonlinear inverse reconstruction for T2 mapping using highly undersampled spin-echo MRI. J Magn Reson Imaging 2011;34:420–428.
12. Marques JP, Kober T, Krueger G, et al. MP2RAGE, a self bias-field corrected sequence for improved segmentation and T1-mapping at high field. NeuroImage 2010;49: 1271–1281.
13. Rao SM, Leo GJ, Bernardin L, Unverzagt F. Cognitive dysfunction in multiple sclerosis. I. Frequency, patterns, and prediction. Neurology 1991;41:685–691.
14. Zigmond AS, Snaith RP. The hospital anxiety and depression scale. Acta Psychiatr Scand 1983;67:361–370.
15. Penner IK, Raselli C, Stocklin M, et al. The Fatigue Scale for Motor and Cognitive Functions (FSMC): validation of a new instrument to assess multiple sclerosis-related fatigue. Mult Scler 2009;15:1509–1517.
16. Kurtzke JF. Rating neurologic impairment in multiple sclerosis: an expanded disability status scale (EDSS). Neurology 1983;33:1444–1452.
17. Fischer JS, Rudick RA, Cutter GR, Reingold SC. The Multiple Sclerosis Functional Composite Measure (MSFC): an integrated approach to MS clinical outcome assessment. National MS Society Clinical Outcomes Assessment Task Force. Mult Scler 1999;5:244–250.
18. Granziera C, Romascano D, Daducci A, et al. Migraineurs without aura show microstructural abnormalities in the cerebellum and frontal lobe. Cerebellum 2013;12:812–818.
19. Granziera C, Daducci A, Simioni S, et al. Micro-structural brain alterations in aviremic HIV+ patients with minor neurocognitive disorders: a multi-contrast study at high field. PLoS One 2013;8:e72547.
20. Granziera C, Daducci A, Romascano D, et al. Structural abnormalities in the thalamus of migraineurs with aura: A multiparametric study at 3 T. Hum Brain Mapp. 2013;12:812–818.
21. Robson PM, Grant AK, Madhuranthakam AJ, et al. Comprehensive quantification of signal-to-noise ratio and g-factor for image-based and k-space-based parallel imaging reconstructions. Magn Reson Med 2008;60:895–907.
22. Wiens CN, Kisch SJ, Willig-Onwuachi JD, McKenzie CA. Computationally rapid method of estimating signal-to-noise ratio for phased array image reconstructions. Magn Reson Med 2011;66:1192–1197.
23. Kober T, Granziera C, Ribes D, et al. MP2RAGE multiple sclerosis magnetic resonance imaging at 3 T. Invest Radiol 2012;47:346–352.
24. Helms G, Draganski B, Frackowiak R, et al. Improved segmentation of deep brain grey matter structures using magnetization transfer (MT) parameter maps. NeuroImage 2009;47:194–198.
25. Yablonskiy DA, Sukstanskii AL, Luo J, Wang X. Voxel spread function method for correction of magnetic field inhomogeneity effects in quantitative gradient-echo-based MRI. Magn Reson Med 2013;70:1283–1292.
26. Fatnassi C, Krueger G, Meuli R, O'Brien KR. 2013. Non linear correction of R2*maps from Macroscopic Field Inhomogeneities. Toulouse, France: ESMRMB.
27. Irarrazabal P, Meyer CH, Nishimura DG, Macovski A. Inhomogeneity correction using an estimated linear field map. Magn Reson Med 1996;35:278–282.

28. An H, Lin W. Impact of intravascular signal on quantitative measures of cerebral oxygen extraction and blood volume under normo- and hypercapnic conditions using an asymmetric spin echo approach. Magn Reson Med 2003;50:708–716.
29. Ogg RJ, Steen RG. Age-related changes in brain T1 are correlated with iron concentration. Magn Reson Med 1998;40:749–753.
30. Schenker C, Meier D, Wichmann W, et al. Age distribution and iron dependency of the T2 relaxation time in the globus pallidus and putamen. Neuroradiology 1993;35:119–124.
31. Ropele S, de Graaf W, Khalil M, et al. MRI assessment of iron deposition in multiple sclerosis. J Magn Reson Imaging 2011;34:13–21.
32. Grossman RI. Magnetization transfer in multiple sclerosis. Ann Neurol 1994;36(Suppl):S97–S99.
33. Klein S, Staring M, Murphy K, et al. elastix: a toolbox for intensity-based medical image registration. IEEE Trans Med Imaging 2010;29:196–205.
34. Roche A, Ribes D, Bach-Cuadra M, Kruger G. On the convergence of EM-like algorithms for image segmentation using Markov random fields. Med Image Anal 2011;15:830–839.
35. Hasan KM, Walimuni IS, Kramer LA, Narayana PA. Human brain iron mapping using atlas-based T2 relaxometry. Magn Reson Med 2012;67:731–739.
36. Georgiades CS, Itoh R, Golay X, et al. MR imaging of the human brain at 1.5 T: regional variations in transverse relaxation rates in the cerebral cortex. AJNR Am J Neuroradiol 2001;22:1732–1737.
37. DeLuca J, Johnson SK, Beldowicz D, Natelson BH. Neuropsychological impairments in chronic fatigue syndrome, multiple sclerosis, and depression. J Neurol Neurosurg Psychiatry 1995;58:38–43.
38. Phillips LJ, Stuifbergen AK. The relevance of depressive symptoms and social support to disability in women with multiple sclerosis or fibromyalgia. Int J Rehabil Res 2010;33:142–150.
39. Osborne JW. Improving your data transformations: applying Box-Cox transformations as a best practice. Pract Assess Res Eval 2010;15:1–9.
40. Haacke EM, Makki M, Ge Y, et al. Characterizing iron deposition in multiple sclerosis lesions using susceptibility weighted imaging. J Magn Reson Imaging 2009;29:537–544.
41. Whittall KP, MacKay AL, Li DK, et al. Normal-appearing white matter in multiple sclerosis has heterogeneous, diffusely prolonged T(2). Magn Reson Med 2002;47:403–408.
42. De Stefano N, Battaglini M, Stromillo ML, et al. Brain damage as detected by magnetization transfer imaging is less pronounced in benign than in early relapsing multiple sclerosis. Brain. 2006;129(Pt 8):2008–2016.
43. Griffin CM, Chard DT, Parker GJ, et al. The relationship between lesion and normal appearing brain tissue abnormalities in early relapsing remitting multiple sclerosis. J Neurol 2002;249:193–199.
44. Vavasour IM, Laule C, Li DK, et al. Is the magnetization transfer ratio a marker for myelin in multiple sclerosis? J Magn Reson Imaging 2011;33:713–718.
45. Rashid W, Hadjiprocopis A, Davies G, et al. Longitudinal evaluation of clinically early relapsing-remitting multiple sclerosis with diffusion tensor imaging. J Neurol 2008;255:390–397.
46. Yu CS, Lin FC, Liu Y, et al. Histogram analysis of diffusion measures in clinically isolated syndromes and relapsing-remitting multiple sclerosis. Eur J Radiol 2008;68:328–334.
47. Moll NM, Rietsch AM, Thomas S, et al. Multiple sclerosis normal-appearing white matter: pathology-imaging correlations. Ann Neurol 2011;70:764–773.
48. Reich DS, Smith SA, Zackowski KM, et al. Multiparametric magnetic resonance imaging analysis of the corticospinal tract in multiple sclerosis. NeuroImage 2007;38:271–279.
49. Hasan KM, Walimuni IS, Abid H, et al. Multi-modal quantitative MRI investigation of brain tissue neurodegeneration in multiple sclerosis. J Magn Reson Imaging 2012;35:1300–1311.
50. Sati P, Cross AH, Luo J, et al. *In vivo* quantitative evaluation of brain tissue damage in multiple sclerosis using gradient echo plural contrast imaging technique. NeuroImage 2010;51:1089–1097.
51. Luo J, Yablonskiy DA, Hildebolt CF, et al. Gradient echo magnetic resonance imaging correlates with clinical measures and allows visualization of veins within multiple sclerosis lesions. Multiple sclerosis. 2013;20: 349–355.
52. Lassmann H. Pathology and disease mechanisms in different stages of multiple sclerosis. J Neurol Sci 2013;333:1–4.
53. Batista S, Zivadinov R, Hoogs M, et al. Basal ganglia, thalamus and neocortical atrophy predicting slowed cognitive processing in multiple sclerosis. J Neurol 2012;259:139–146.
54. Nielsen AS, Kinkel RP, Madigan N, et al. Contribution of cortical lesion subtypes at 7T MRI to physical and cognitive performance in MS. Neurology 2013;81:641–649.

Supporting Information

Additional Supporting Information may be found in the online version of this article:

Data S1. Supplementary data.

